EFFICIENT SHAPE OPTIMIZATION IN AERONAUTICS: INTEGRATING PARAMETRIC CAD AND MESH MORPHING FOR ENHANCED AERODYNAMIC PERFORMANCE

Lopez A[1], Magri G[2], Cella U[1], Urso G[3], Della Barba F[2] & Biancolini M E[1]

[1]Università di Roma, Tor Vergata
[2]Università degli studi di Padova
[3]RBF Morph srl, Monte Compatri (RM)

Abstract

Shape optimization is critical in aeronautics, especially with increasing electrification, necessitating reduced consumption and enhanced aerodynamic performance to extend aircraft range. Additionally, reducing computation times is vital due to the lengthy durations of Computational Fluid Dynamics (CFD) simulations and the need for multiple simulations to create a significant dataset for shape optimization or Reduced Order Model (ROM) building.
This paper proposes an innovative optimization workflow that combines the benefits of two key established methods: parametric Computer-Aided Design (CAD) and mesh morphing. The approach involves the use of a scriptable CAD editor, in this study we used the opensource ESP (Engineering Sketch Pad), to generate Design Points (DPs). By comparing the baseline CAD with its generated variation, a cloud of points is created, which can be employed to deform the computational grid using a mesh morphing technique based on Radial Basis Functions (RBF). The workflow is fully automated to explore multiple DPs and has been applied to the Boeing 787 inspired OPAM (Open Parametric Aircraft Model) getting promising results in terms of efficiency improvement. The proposed workflow represents a highly innovative and cost-effective solution to the problem of automatic mesh generation methods: instead of creating a new mesh, the pre-existing mesh is deformed but according to the modifications dictated by the CAD editor.

Keywords: Parametric CAD, Mesh Morphing, RBF, Optimization, CFD

1. Introduction

Optimization workflows can be broadly categorized into two main types: methods based on parametric CAD [1][2][4] and methods based on mesh morphing [5][6][7][20]. Both approaches have their advantages and drawbacks. Utilizing parametric CAD methods generally provides greater control over shape variations by directly manipulating the mathematics governing surface and volume generation. The primary limitation of these methods is the need to generate a new mesh for each DP, a time-consuming and labor-intensive step that is challenging to automate while ensuring mesh quality.

On the other hand, mesh morphing-based methods offer significant advantages. Notably, there is no requirement to create a new mesh for each DP, leading to a substantial reduction in computational times associated with mesh generation and the convergence of each DP. The baseline solution at convergence can be leveraged to expedite the solution for each DP. Importantly, the mesh topology remains unchanged, a crucial aspect for creating ROMs [8][9]. Furthermore, mesh morphing enables advanced optimization workflows that employ the adjoint method to identify the optimal combination of input parameters [10][11], along with analyses such as modal transient fluid-structure interaction (FSI) [12].

However, mesh morphing methods come with their limitations, including less control over shape variations and the necessity to re-create a new CAD model that reproduces the optimized shape at

the end of the process. To overtake the limitations of both methods, we propose in this paper a hybrid method that combines their benefits. The devised workflow was used to optimize the efficiency of OPAM [3], a parametric model inspired by the Boeing 787 proposed in the second GMGW (Geometry and Mesh Generation Workshops) [23]. The simplified model (Figure 1) is based on 53 adjustable design parameters, with a scale of approximatively 1:300 with respect to B787. The workshop challenge involved starting with a parametric CAD model and developing an automatic meshing procedure that preserves mesh quality for each DP [15]. In this new study, the challenge was approached from a different perspective. Instead of generating the mesh for each DP, the CAD modification is transferred to the mesh, and the baseline mesh is deformed accordingly. This approach offers a substantial computational advantages and makes the workflow suitable for generating Reduced Order Models (ROMs), thanks to the preserved mesh topology of new shape variations.

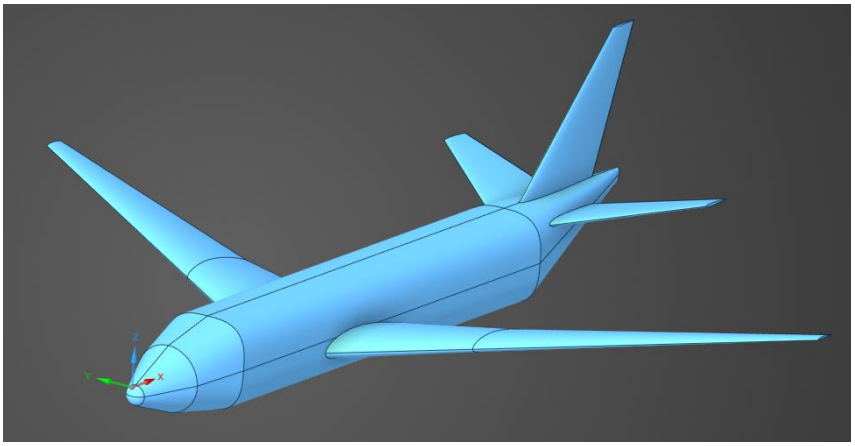

Figure 1: The OPAM baseline

2. Methods

To identify the optimum, a classical response surface methodology [13] was used, creating a Design of Experiment (DOE) with the Latin Hypercube algorithm [14]. A hybrid method was employed, combining the benefits of mesh morphing and parametric CAD. Specifically, the parameters are defined in a Python script that generates the CAD. Each CAD variant is then compared with the baseline, creating a cloud of points that spans from the initial state to the new CAD. This point cloud is used as an RBF field to translate the information from the CAD level to the mesh level. Finally, the mesh is deformed and a CFD simulation is run for each DP. Figure 2 schematizes the workflow followed in this study.

Figure 2: Hybrid workflow

2.1. CAD generation

For the generation of parametric CAD [23], an opensource CAD editor was employed: ESP. The workflow exhibits remarkable flexibility and is easily customizable for integration with various CAD editors. ESP is a browser-based design software designed for creating, modifying, and generating three-dimensional solid models. The tool uses OpenCascade as the engine for geometry generation and reads input ASCII files containing parameters and calls the necessary functions to generate the CAD. In this case, it is necessary to script the modification of these ASCII files. The tool has a graphical interface but can also be launched in batch mode.

2.2. Cloud of points generation

One of the critical steps in the workflow is the transfer of information from CAD to the mesh. A routine

is required to encode the shape variation defined on the geometry, making it usable for mesh deformation. For this operation, a tool was developed to create a point cloud on the surface of the baseline geometry and a series of corresponding points on the CAD variant. Several challenges arise in this operation. One fundamental aspect is the recognition of homologous surfaces and edges. Using scriptable CAD editors is a significant advantage in this regard. The same operations are executed sequentially by changing the input parameters, ensuring that the order of generated surfaces and edges remains consistent. For the successful coupling of homologous entities on different CADs, it is necessary for the CADs to be iso-topological with entities indexes preserved.

Another critical aspect is generating homologous points on homologous surfaces and edges. The surfaces are covered with a regular grid of points in the two-dimensional U-V space, and similarly, the edges are covered with a set of one-dimensional points evenly spaced. Since the number of points is the same between the two clouds, the grids can be put into one-to-one correspondence. Finally, another critical aspect is managing the interface zone between two surfaces. To ensure good mesh quality and proper overlap of the deformed mesh with the corresponding geometry, points on edges and surfaces are independently defined, and a buffer is provided between them. Figures 3, 4, and 5 illustrate the steps of this workflow applied to a simple case (NACA profile). First, a CAD variant is created using a script. The CAD variant is compared with the baseline, and a point cloud is generated, spanning from the initial state to the new one. At this stage, point spacing and buffer are checked (Figure 4).

Once the two points clouds are created, they are read as RBF points and displacements for interpolation. Consequently, they can be used to deform the mesh.

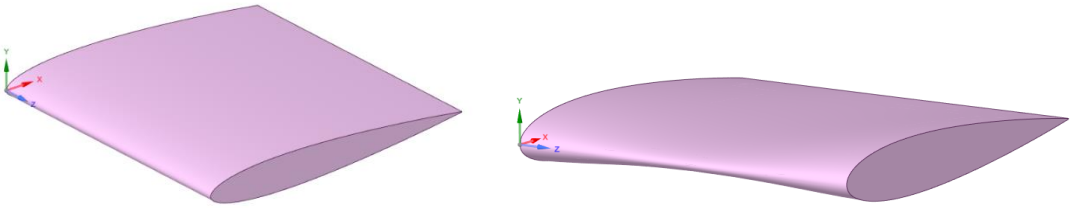

Figure 3: Example of NACA profiles (baseline-left and deformed-right)

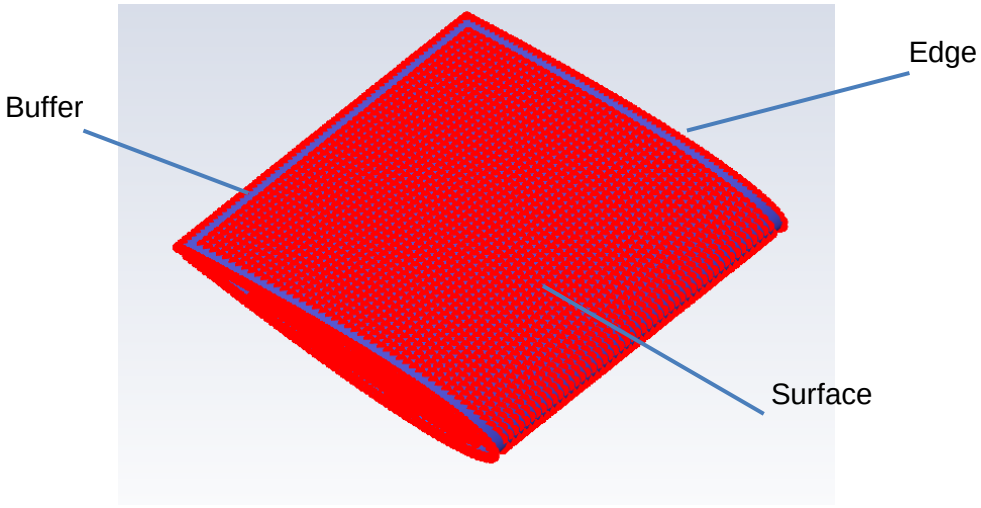

Figure 4: Cloud of points generated on the baseline

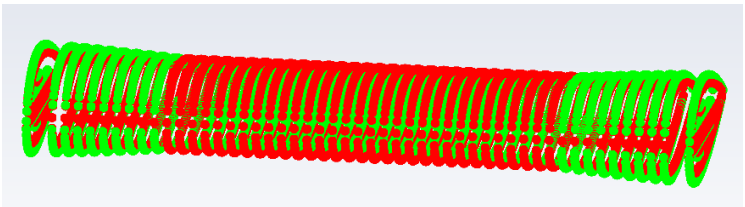

Figure 5: Comparison of points on the baseline (red) and on the deformed geometry (green)

2.3. RBF Mesh morphing

In this workflow, a mesh morphing technique based on RBFs was utilized to update each DP [16][17][18][19][22]. Specifically, the point clouds were translated into an RBF field as source points of the RBF problem. This process effectively translates the parametrization defined at the CAD level to the mesh level.

In mathematical terms [5], a RBF is a real-valued function whose value depends solely on the distance between the function's argument and a point in the defined domain. RBFs find their natural application in mesh morphing. The concept involves defining parametric displacements to deform the pre-existing mesh. RBFs are employed to interpolate these defined displacements onto the mesh nodes. Source points are established, and a known displacement is applied. Displacements are then interpolated on the mesh nodes using a proximity criterion: displacements proportional to the distance from the surrounding source points are applied to the mesh nodes. The full field is obtained repeating the RBF interpolation for each direction:

$$f^x(x) = \sum_{i=1}^{m} \gamma_i^x \phi(\|c_i - x\|) + \beta_1^x + \beta_2^x x_1 + \beta_3^x x_2 + \beta_4^x x_3 \quad (1)$$

$$f^y(x) = \sum_{i=1}^{m} \gamma_i^y \phi(\|c_i - x\|) + \beta_1^y + \beta_2^y x_1 + \beta_3^y x_2 + \beta_4^y x_3 \quad (2)$$

$$f^z(x) = \sum_{i=1}^{m} \gamma_i^z \phi(\|c_i - x\|) + \beta_1^z + \beta_2^z x_1 + \beta_3^z x_2 + \beta_4^z x_3 \quad (3)$$

In the equation, γ represents the weights, and ϕ stands for the radial function, with the polynomial term serving as a stabilizing function. The solution to the system involves applying boundary conditions, which include the known displacement values at the source points and ensuring the orthogonality of the coefficients. Various RBFs are at our disposal, each offering different interpolation behaviors. While ensuring the prescribed values at the center points, the specific RBF choice influences the overall interpolation behavior. It's important to note that the computational cost and solution approaches to RBFs may differ based on the selected type of function.

For the example case shown earlier (NACA profile), Figures 6 and 7 show how the mesh is deformed and how it perfectly follows the deformed CAD.

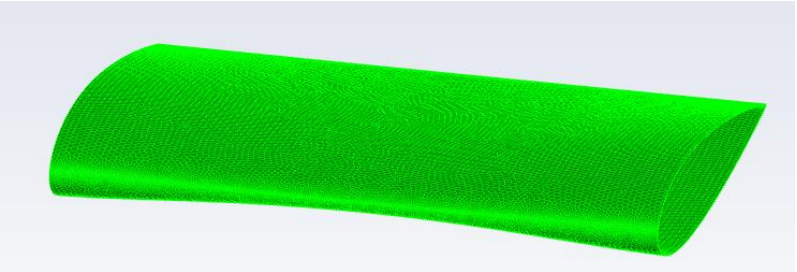

Figure 6: Deformed mesh

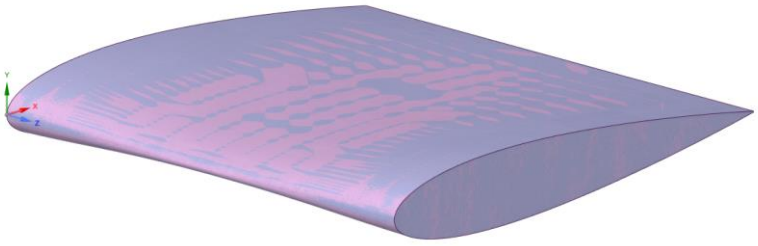

Figure 7: Comparison of deformed mesh and deformed CAD

2.4. Mesh and setting

The first step was to define the baseline and create the mesh of the initial geometry. Table 1 outlines the main characteristics of the mesh, and Figure 9 provides some details of the mesh. Symmetry was leveraged to reduce the computational domain.

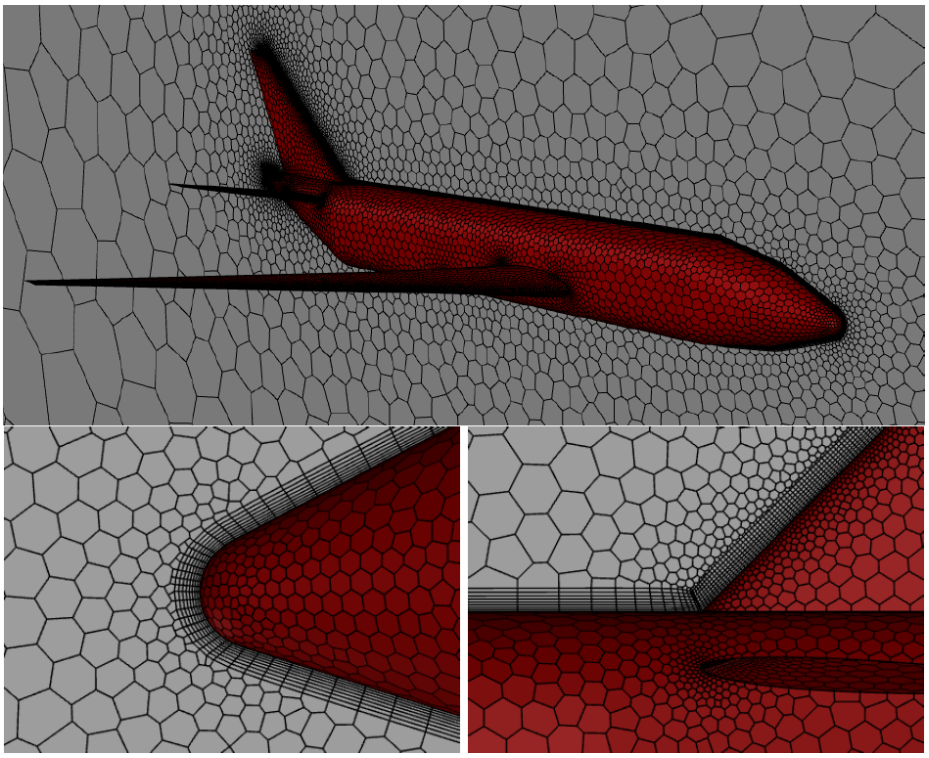

Figure 9: Mesh baseline

Table 1: Main mesh statistics

Number of faces	*2199081*
Number of cells	*425052*
Number of nodes	*1479730*
Max. Skewness	*0.8998*
Min. Orthogonal Quality	*0.1002*
Max. Aspect Ratio	*43.9261*
y+	*<1*

An instantaneous altitude of 7000 feet is presumed. The flow is characterized by Re = 1.3×10^6
The following main options are configured:

- Steady-state simulation;
- Density-based solver;
- k-omega SST turbulence model;
- Air as an ideal gas with the Sutherland viscosity law;
- Boundary conditions:
  - Inlet [pressure-far-field]: Airflow velocity of 120 m/s (Mach equal to 0.36) inclined by α = 4.8°. Pressure and temperature relative to the established altitude.
  - Outlet [pressure-outlet]: Pressure and temperature relative to the established altitude.
  - Side [pressure-far-field]: Same conditions as the Inlet.
  - Symmetry [symmetry]: Symmetry plane.
  - Aircraft surface [wall].

The implicit Roe-FDS formulation with second-order discretization was employed.

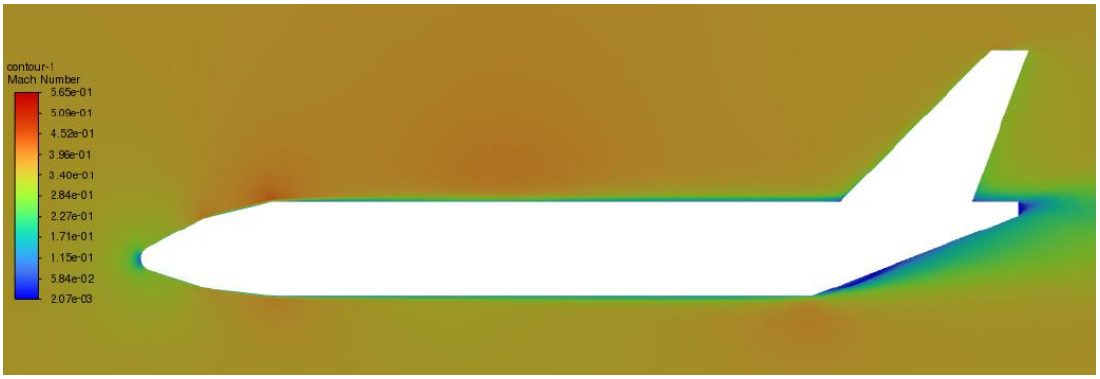

Figure 10: Velocity contour on the symmetry plane

2.5. Shape parameters and DOE

For the sampling, the Latin Hypercube Sampling (LHS) method was employed. LHS is a statistical technique for the random generation of parameter values. This method can significantly reduce the number of executions required to achieve a reasonably accurate result.

Five reference parameters were selected for use:

- Wing aspect ratio with a fixed surface, indicated by parameter P1 - *wing:aspect*
- Ratio of profile thickness to root chord of the wing: P2 - *wing:thickr*
- Position of the wing root in the longitudinal direction, through parameter P3 - *wing:xroot*
- Angle of incidence of the profile at the section dividing the wing between the outer and inner zones, indicated by P4 - *wing:alphab*
- Power of the super-ellipse of the central fuselage, with parameter P5 - *fuse:power*

The values of these 5 parameters were varied within specified limits (Table 3) and 52 DPs were generated.

Table 1: Range of variation of each parameter

Parameter	**Nominal Value**	**Lower Value**	**Upper Value**
wing:aspect P1	*9*	*7*	*11*
wing:thickr P2	*0.15*	*0.1*	*0.2*
wing:xroot P3	*54*	*51*	*57*
wing:alphab P4	*2°*	*1°*	*3°*
fuse:power P5	*3*	*2*	*4*

3. Results

For each DP, the workflow described in the previous section is utilized. The deformed CAD is created by updating the input parameter values with ESP, generating the RBF point cloud from the baseline to the new configuration, deforming the mesh, conducting the analysis, and saving the aerodynamic efficiency value, which is the observable of interest.

Once all DPs are executed, the DOE is updated with the output values, and response surfaces are generated to identify the optimal solution.

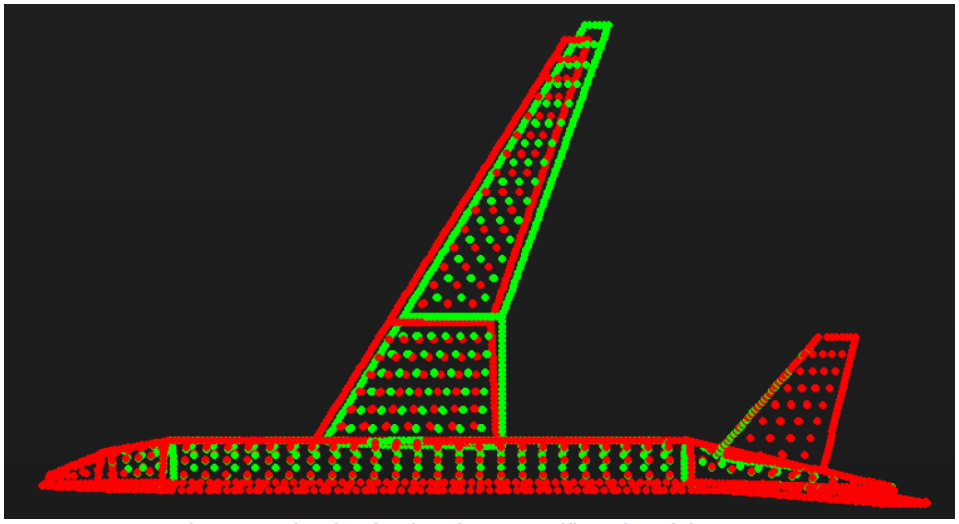

Figure 2: Clouds of points for a specific point of the DOE

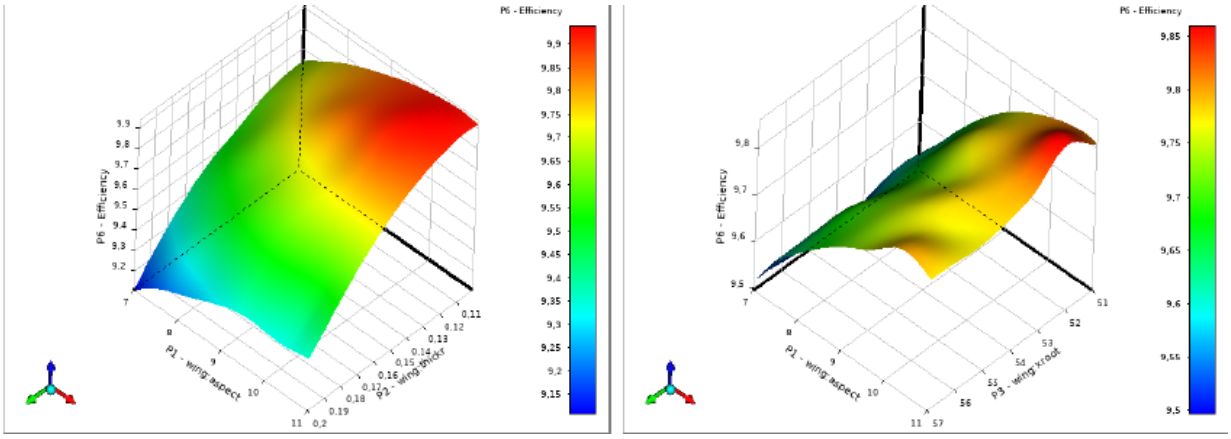

Figure 3: Examples of response surfaces

The optimal geometry according to the candidate points has a wing aspect ratio slightly below the imposed maximum. Indeed, this parameter influences the induced drag coefficient.

However, wings with a high aspect ratio are not structurally straightforward. Additionally, as wing area increases, the aircraft becomes more sensitive to gusts.

Ultimately, it can be asserted that a higher aspect ratio is an expected result. Intuitively, a more cylindrical and aerodynamic fuselage was also anticipated; hence, the power of the proposed super-ellipse is set to 2. The longitudinal position of the wing does not deviate excessively from the original value. On the contrary, both the angle of incidence of the mid-wing profile and the thickness of the profile at the root take on values close to the lower limits. In conclusion, the influence of these parameters on aerodynamic efficiency is evident in the image below.

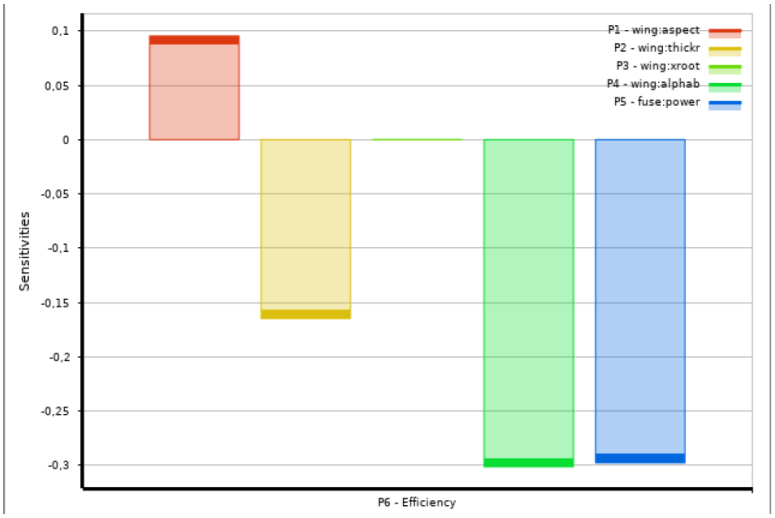

Figure 4: Parameters sensitivity

Once the optimization procedure is complete, the first candidate point is examined. The optimal geometry is generated by launching the ESP terminal with the appropriate updated parameters.

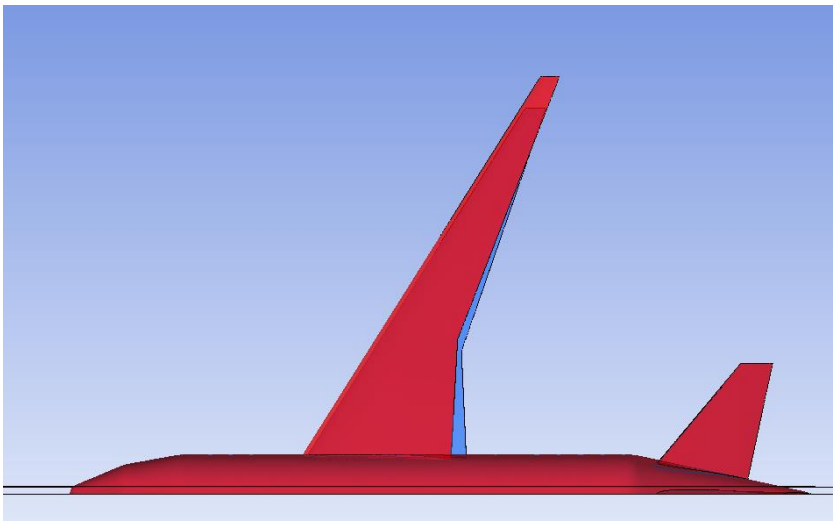

Figure 5: Comparison of baseline (blue) and optimized shape (red)

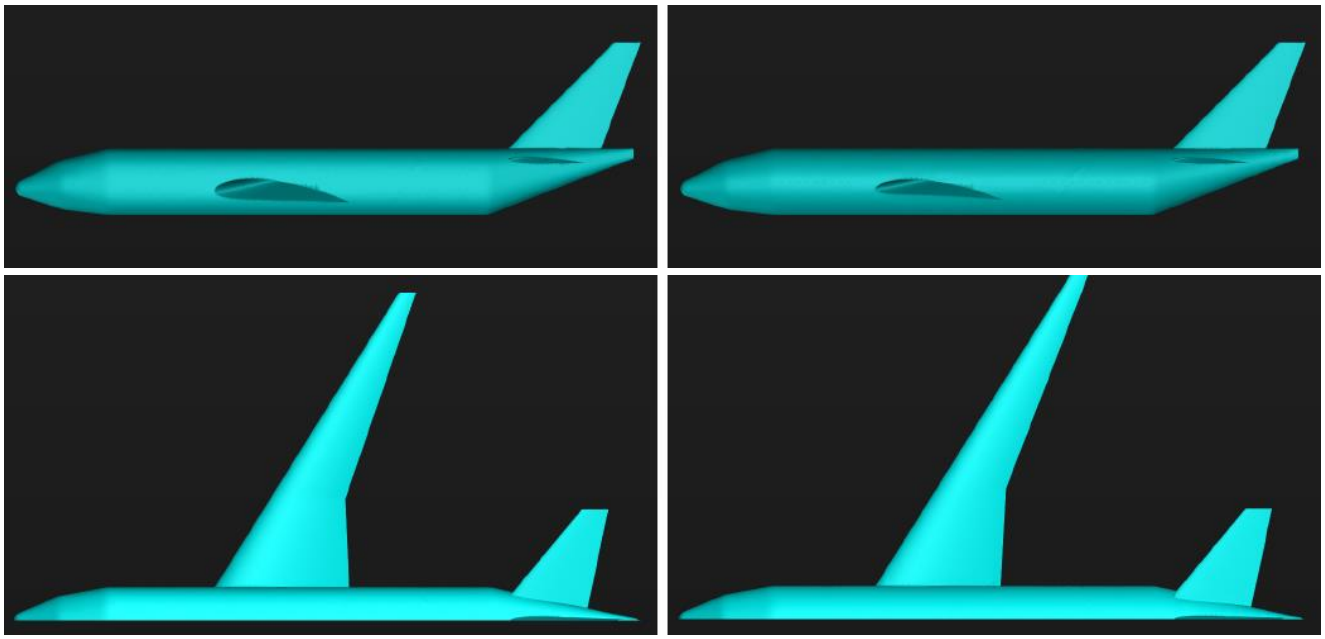

Figure 6: Comparison of baseline (left) and optimized shape (right)

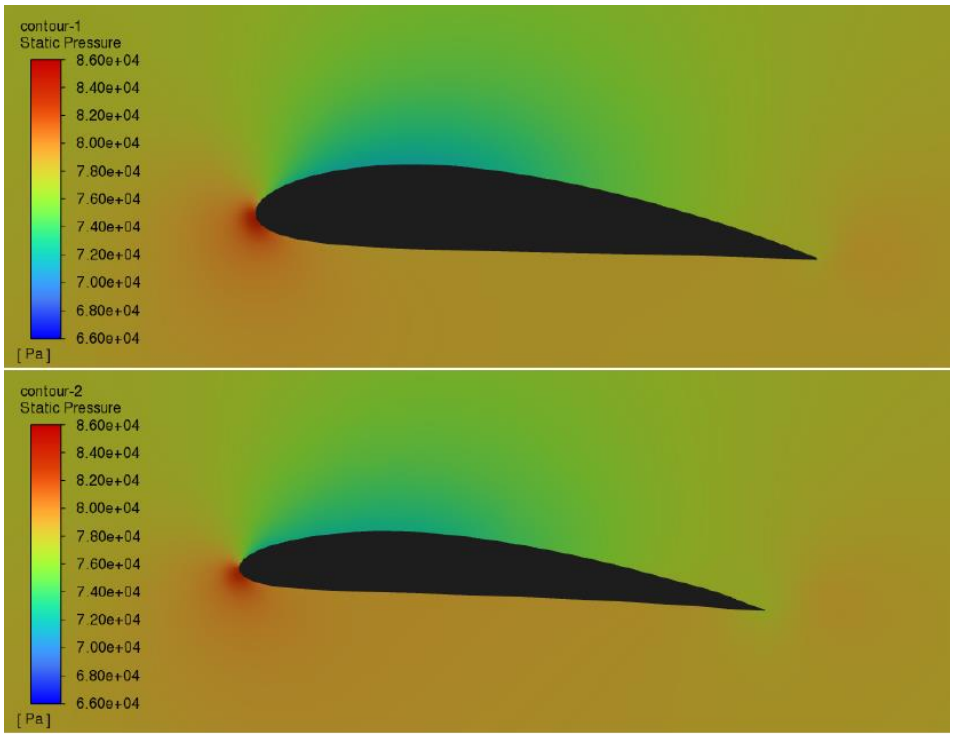

Figure 7: Comparison of pressure field of baseline (above) and optimized (below)

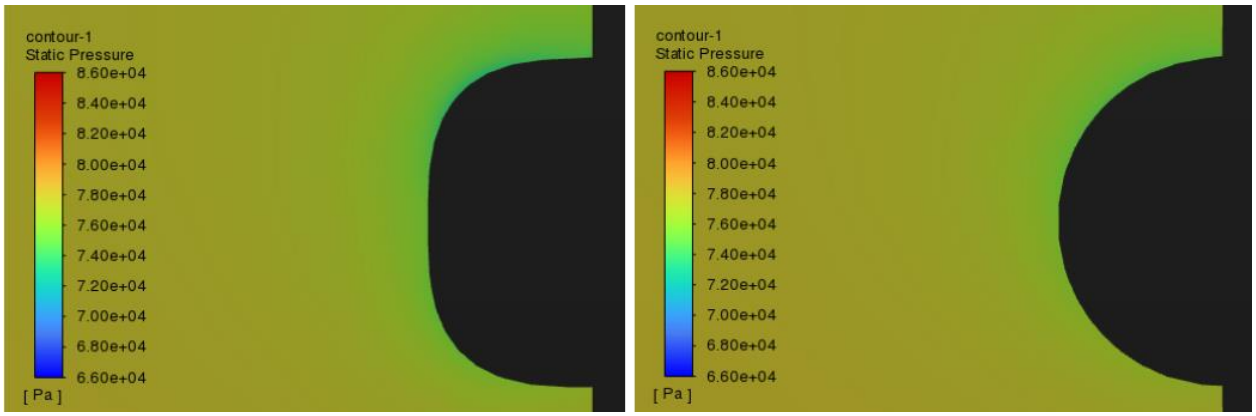

Figure 8: Comparison of pressure field of baseline (left) and optimized (right)

The change in fuselage shape allows for a reduction in drag force; the cylindrical shape becomes more streamlined and aerodynamic. The wing has a smaller frontal area, and separation zones on the upper part are less extensive. The value predicted by the response surfaces for efficiency is 10.21, very close to the value of 10.28 obtained from the CFD analysis. Therefore, the number of DPs is sufficiently high to construct a reliable and accurate model that identifies the optimum. The increase in efficiency is 5.1%.

4. Conclusions

In this study, an integrated workflow was proposed, combining the benefits of mesh morphing and CAD parameterization. This approach ensures greater control in defining parameters (which are specified on the CAD) while using mesh morphing to update the mesh, thereby accelerating computational times. The proposed work aims to develop a fully automated workflow where shape modifications are transferred from the geometry to the mesh, which is deformed using RBF to interpolate displacements on the mesh nodes. OPAM was chosen as a use-case. The idea is to have a parametric model of an entire aircraft defined by a sufficiently comprehensive

parameterization capable of exhaustively characterizing its design. The proposed workflow represents a cost-effective solution to the problem of automatic mesh generation methods. Instead of creating a new mesh, the pre-existing mesh is deformed according to the modifications dictated by the CAD editor.

The results are highly encouraging, particularly in terms of the mesh quality obtained for each DP and the integration of various tools into a single automated workflow. The optimization results are also noteworthy, with an approximately 5% increase in efficiency.

Proposed approach makes feasible ROMs or adjoint-based workflows, for which it is essential that the mesh topology remains unchanged, a task that is nearly impossible with automatic mesh generation tools. Future developments are in fact focused on building ROM models [21][24][25] where training snapshots are generated using this workflow with the ambition to create a platform for real-time visualization of field quantities, where the CAD is directly linked to CFD results.

References

[1] https://cadquery.readthedocs.io/en/latest/intro.html

[2] Trifari V, De Marco A, Di Stasio M, Ruocco M, Nicolosi F, Grazioso G, Ahuja V and Hartfield R *An aircraft design workflow using the automatic knowledge-based modelling tool JPAD Modeller: AIAA 2022*

[3] Woeber C, Masters J S and McDaniel D R, *Summary of Exascale and Remeshing Efforts for the Second Geometry and Mesh Generation Workshop: AIAA 2019*

[4] Park C, Joh C Y & Kim Y S, *Multidisciplinary design optimization of a structurally nonlinear aircraft wing via parametric modeling: International Journal of Precision Engineering and Manufacturing 2009*

[5] Biancolini M E *Fast Radial Basis Functions for Engineering Applications*, *2017*

[6] Andrejašič M , Eržen D , Costa E , Porziani S ,Biancolini M E , Growt C *mesh morphing based FSI method used in aeronautical optimization applications: ECCOMAS 2016*

[7] Biancolini M E, Cella U, *Springer: Flexible Engineering Toward Green Aircraft, 2020*

[8] Biancolini M E, Capellini K, Costa E, Growth C & Celi S, Fast interactive CFD evaluation of hemodynamics assisted by RBF mesh morphing and *reduced order models: the case of aTAA modelling, International Journal on Interactive Design and Manufacturing (IJIDeM), 2020*

[9] Castronovo P, Mastroddi F, Stella F & Biancolini M E, *Assessment and development of a ROM for linearized aeroelastic analyses of aerospace vehicles, CEAS Aeronautical Journal, 2017*

[10] Lopez A *Ottimizzazione di flussi esterni ed interni mediante metodi CFD adjoint e mesh morphing* 2021

[11] Kapsoulis D H, Asouti V G, Giannakoglou K C, Porziani S, Costa E, Groth C, Cella U and Biancolini M E, *Evolutionary aerodynamic shape optimization through the RBF4AERO platform, ECCOMAS 2016*

[12] Di Domenico N, Groth C, Wade A, Berg T, Biancolini M E, *Fluid structure interaction analysis: vortex shedding induced vibrations, AIAS 2017*

[13] Zhixin Xu , Dongqin Xia , Nuo Yong , Jinkai Wang , Jian Lin , Feipeng Wang ,Song Xu , and Daochuan Ge, Applied Sciences 2023, Hybrid Particle Swarm Optimization for High-Dimensional Latin Hypercube Design Problem

[14] Prapatsorn Borisut, Processes 2023, *Adaptive Latin Hypercube Sampling for a Surrogate-Based Optimization with Artificial Neural Network*

[15] https://www.rbf-morph.com/rbf-morph-at-geometry-and-mesh-generation-workshop/

[16] Birgit Saalfeld, Markus Rutten, Stefan Saalfeld and Jens Kunemund, ECCOMAS 2012, *Improved mesh morphing based on radial basis functions*.

[17] Daniel Sieger, Stefan Menzel & Mario Botsch, *High Quality Mesh Morphing Using Triharmonic Radial Basis Functions*, Proceedings of the 21st International Meshing Roundtable

[18] Flavio Gagliardi, Kyriakos C. Giannakoglou, *RBF-based morphing of B-Rep models for use in aerodynamic shape optimization*, Advances in Engineering Software 2019

[19] Luca Abergo, Myles Morelli, Alberto Guardone, *Aerodynamic shape optimization based on discrete adjoint and RBF*, Journal of Computational Physics 2023

[20] Christian B. Allen & Thomas C. S. Rendall, *CFD-based optimization of hovering rotors using radial basis functions for shape parameterization and mesh deformation*, Optimization and Engineering 2013

[21] Nicola Demo, Marco Tezzele, Andrea Mola and Gianluigi Rozza, *Hull Shape Design Optimization with Parameter Space and Model Reductions, and Self-Learning Mesh Morphing,* Journal of Marine Science and Engineering 2021

[22] Ismail Bello & Shahrokh Shahpar, *Mesh Morphing for Turbomachinery Applications Using Radial Basis Functions*, 27th International Meshing Roundtable

[23] John F. Dannenhoffer, *Analysis of GMGW2 Case 3: Design Variations*, GMGW2

[24] Yidong Lang, Stephen E. Zitney, Lorenz T. Biegler, *Optimization of IGCC processes with reduced order CFD models*, Computers & Chemical Engineering 2011

[25] Amsallem, D., Farhat, C. *On the Stability of Reduced-Order Linearized Computational Fluid Dynamics Models Based on POD and Galerkin Projection: Descriptor vs Non-Descriptor Forms.* In: Quarteroni, A., Rozza, G. (eds) Reduced Order Methods for Modeling and Computational Reduction. MS&A - Modeling, Simulation and Applications, vol 9. Springer, 2014